Convective precipitation trends in the Spanish Mediterranean region

María Carmen Llasat [a,*], Anna del Moral [a], Maria Cortès [a,c], Tomeu Rigo [b]

[a] *GAMA, Department of Applied Physics, University of Barcelona, Barcelona, Spain*
[b] *Meteorological Service of Catalonia, Barcelona, Spain*
[c] *AEMET, Barcelona, Spain*

ARTICLE INFO

ABSTRACT

This paper aims to analyse the distribution and temporal evolution of convective precipitation in the Mediterranean region of Spain. To accomplish this goal, we used 148 sets of 5-min rainfall rate data from the 1989–2015 period. The selected regions were the Júcar Hydrographic Confederation (CHJ) and the Internal Basins of Catalonia (CIC), which cover most of the autonomous communities of Catalonia and the Valencian Community (east Spain). The average 5-min intensity threshold of 35 mm/h and the β parameter, defined as the ratio between convective precipitation versus total precipitation in any period, were used to characterise convective precipitation. Convective episodes were categorised as "very convective", "moderately convective", and "slightly convective" based on the β value. After quality control, the series of 129 stations were clustered into homogeneous precipitation zones that also include β as one of the variables of characterisation. The results show that convective precipitation can contribute to total annual precipitation by up to 16% on average, but it is generated by a very small percentage of convective events (between 3% and 6% across all the stations) in comparison with the total number of rainfall episodes. In this sense, moderately convective events are the most common, with a predominantly unimodal monthly distribution of β, with summer the most convective season. Trends show a significant increase in precipitation, convective precipitation, and convective episodes in the CHJ. On the other hand, a positive trend of convective events is predominant in the CIC region, despite an overall precipitation decrease in the analysed period. These results are relevant given that extreme daily rainfall does not show a positive or significant trend, and they are in line with the impact of climate change on increased atmospheric instability and water vapour in the atmosphere. They highlight the need to work with sub-daily precipitation series in the case of the Mediterranean, which is mainly affected by flash floods.

1. Introduction

One of the main impacts of climate change appears to be an increase in heavy precipitation, as pointed out by the Clausius-Clapeyron equation (Alexander et al., 2006). Some works analyse the mechanisms that could be the cause of the increase in precipitation intensity associated with a warmer atmosphere (Lenderink and van Meijgaard, 2008; Berg and Haerter, 2013). For instance, Ye et al. (1998), Chou et al. (2012) and Lepore et al. (2015) put the increase in convective precipitation behind the increase in CAPE (Convective Available Potential Energy, Weisman and Klemp, 1986) in response to warming and an increase in water vapour in the atmospheric boundary layer. Along the same line, Westra et al. (2014) also point towards an increase in the intensity in convective precipitation due to more water vapour, which intensifies the convective process. Ye et al. (2017) found an increase of the convective

precipitation over Eurasia for the 1966–2000 period in 61.8% of the analysed stations. Recently, Wu et al. (2019) have suggested that the strong Urban Heat Island (UHI) effect in large urban agglomerations is conducive to intensified hourly precipitation as a result of the individual and combined effects of land cover and land use changes, and an increase in anthropogenic aerosol emissions.

However, most of these works use a conceptual approach or different type of proxy data to identify convective precipitation. For instance, Berg et al. (2013) analysed convective precipitation in Germany for the 1971–1987 period based on the Extended Edited Synoptic Cloud Report Archive (EECRA) synoptic classification. Most of the existing works focus more on the physical aspects of meteorological processes (Schumacher and Houze Jr., 2003; Houze Jr et al., 2007; de Leon et al., 2016). One such example is a recent contribution by Francipane et al. (2020) who proposes an algorithm based on a variant of a k-means clustering
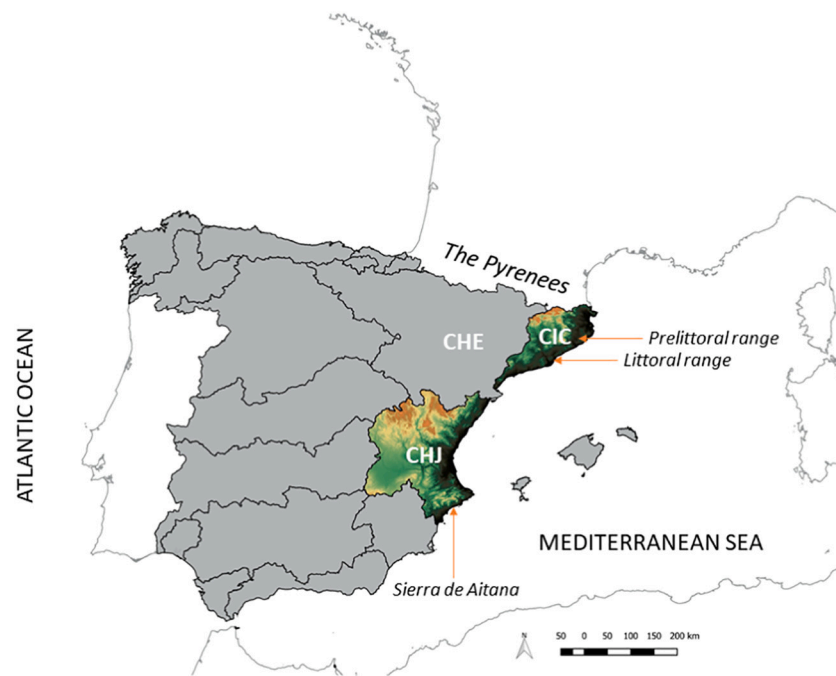

Fig. 1. Map of Peninsular Spain and the Balearic Islands showing the hydrographic basins. The area of study also shows the orography. CIC: Internal Basins of Catalonia; CHJ: Júcar Hydrographic Confederation; CHE: Ebro Hydrographic Confederation. The locations of the Coastal and Pre-Coastal ranges (CIC) and the Aitana mountain range (CHJ) are also shown.

and Principal Component Analysis (Adelfio et al., 2011), which is able to classify precipitation type, distinguishing between convective and stratiform components. Ye et al. (2017) used 3-hourly synoptic weather observations and daily precipitation records from 152 stations, the latter including information on precipitation characteristics, provided by weather spotters. In this paper, convective precipitation is identified manually and includes "rain showers" and thunderstorms. Since precipitation is recorded on a daily scale, all the accumulated daily precipitation is identified as convective, non-convective, or mixed precipitation. This can justify the high trend of convective precipitation found by the authors in some stations, which can reach more than 130 mm per decade. The distinction between convective and stratiform precipitation was based on Houze (1977) and, in a more restrictive way, was also applied by Rice and Holmberg (1973) and Llasat and Puigcerver (1985), who identified convective precipitation with the rainfall produced during thunderstorms. Llasat and Puigcerver (1997) added to this criterion the hyetograph shape from the "Jardí" pluviography instantaneous rainfall rate strip charts. This pluviograph was located near the city of Barcelona (Jardí, 1921; Puigcerver et al., 1986) and, after being digitalised, it was possible to associate 0.8 mm/min intensity rates to convective precipitation. This value was near the threshold of 50 mm/h proposed by Dutton and Dougherty (1979) and Watson et al. (1982) when they analysed the impact of precipitation intensity on telecommunications. The advantage of setting this threshold lies in the possibility of being able to see the evolution of convective precipitation throughout the day or within the precipitation episode itself.

Llasat (2001) modified the threshold to agree with current databases and proposed the value of 35 mm/h for a 5-min rainfall rate series. The application of this criterion to the 1927–1981 series of rainfall intensities provided by the Jardí pluviography led to a distinction between events based on the β value. This value is defined as the ratio between precipitation with a greater intensity than the aforementioned threshold (35 mm/h for 5-min rainfall rates), and the total precipitation amount recorded for the event. Then, it was possible to distinguish between "very convective events" (β_1), "moderately convective events" (β_2), and "slightly convective events" (β_3), depending on the convective contribution to total precipitation ($\beta \geq 80\%$, $80\% > \beta \geq 30\%$ and $30\% > \beta > 0$,

respectively). This classification can also be related to other features of the event, such as the precipitating system, the hyetograph design, or the impacts (Llasat et al., 2016). In this way, local flash floods were usually associated with "very convective events" produced by isolated cells and multicellular systems. On the other hand, and as a result of their longer duration, extended flash floods, or multiple flash-floods in different catchments as a consequence of the same event, were caused by "moderately convective events" associated with more organised systems, such as mesoscale convective systems (MCS) (Schumacher and Johnson, 2005; Rigo et al., 2019). Finally, large floods require precipitation of a longer duration and extension, with heavy convective events, and are consequently classified as "slightly convective events". In this case, these events were caused by convective precipitation embedded in stratiform systems (Llasat et al., 2016). Therefore, in a situation with an increase in very convective or moderately convective events, it is possible that the series of extremes like ETCCDI (Expert Team on Climate Change Detection and Indices), retrieved on a daily scale, would not detect it.

Previous works show that no trends have been detected in Catalonia, neither in terms of extreme precipitation values on a daily scale nor on the associated ETCCDI index (Turco and Llasat, 2011; Llasat et al., 2016). However, Llasat et al. (2016) found an increase in convective precipitation in the Internal Basins of Catalonia (northeast Spain) for the 1996–2011 period that would be concentrated in fewer, but more intense, torrential events. Keeping in mind that this increase would be the only current sign to justify the impact of climatic change on torrential precipitation in this region, the objective of this paper is to analyse the evolution of convective precipitation over a more extended period and region.

This paper deals with the analysis of a 5-min rainfall rate series for the majority of the Mediterranean region on the Iberian Peninsula, in order to find any potential trends in convective precipitation or in different types of convective events. With this aim in mind, the paper starts by presenting the data and region of study, breaking down different areas based on their precipitation features, followed by the criteria and methodology used. Afterwards, there is a systematic analysis of all the potential trends related to convective precipitation.
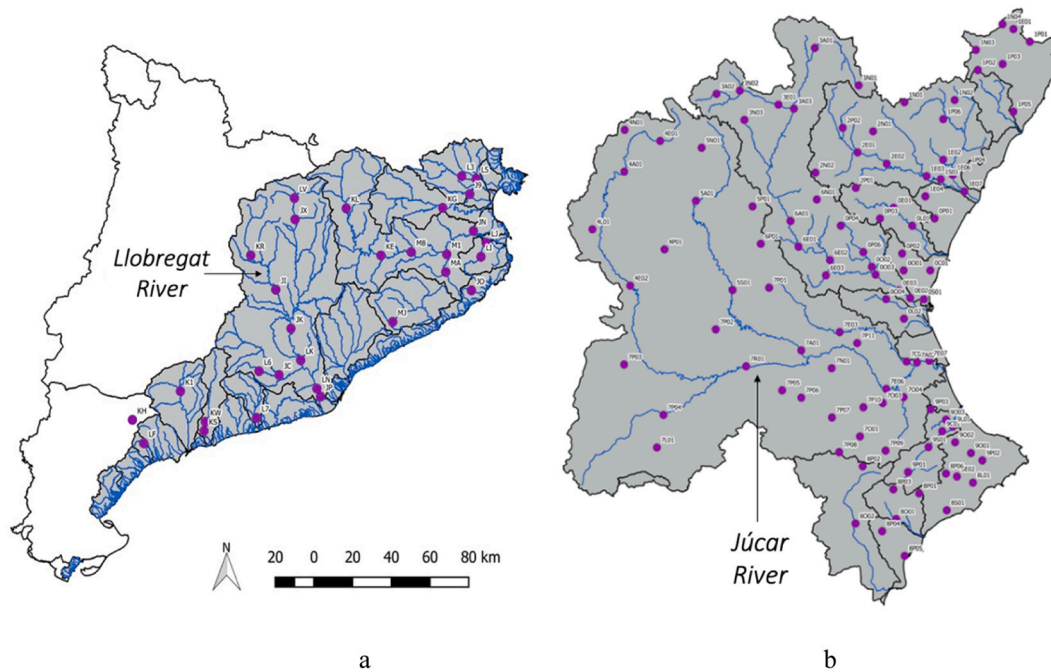
Fig. 2. Sub-catchments of the Internal Basins of Catalonia (2a) and the Júcar Hydrographic Confederation (2b). The rain gauges selected for this study are shown.

Finally, the paper ends with the Conclusions and Discussion section.

2. Data and region of study

Fig. 1 shows the region of study, which is made up of the Internal Basins of Catalonia ("*Conques Internes de Catalunya*", CIC) and the Júcar Hydrographic Confederation ("*Confederación Hidrográfica del Júcar*", CHJ). The CIC has an extension of around 16,000 km^2 and includes 27 sub-catchments, of which the Llobregat Basin is the largest (4957 km^2) (Fig. 2a). The region is bordered to the east by the Mediterranean Sea, with a coast running from southeast to northeast; it is bordered by the Pyrenees to the north, running from west to east, with altitudes over 2000 m; and bordered to the west and south by the Ebro Basin. Running parallel to the coast, the Coastal (600 m) and Pre-Coastal mountain ranges (1800 m) are crucial to the development of convective clouds, triggering the potential instability at low levels that characterise this region (mainly with wet and warm advection from the southeast), or creating the favourable conditions for the systems to remain stable (Llasat, 2009). The presence of the Pyrenees can also lead to remarkable effects on mesoscale pressure distribution, giving rise to processes such as convergence lines and orographic dipoles. For example, the flood event of October 1987, when more than 400 mm were recorded in 24 h near Barcelona, was favoured by a meso-high created in the south Pyrenees (Ramis et al., 1994).

Thirty 5-min rainfall gauge stations from the SAIH (Automatic Hydrological Information System) network belonging to the Catalan Water Agency were selected for 1996–2015 period (20 years). This network was created in 1996 and has been extensively used to analyse specific flood events (Llasat et al., 2003), the rainfall regionalisation of the CIC (Llasat et al., 2007) and the calibration of radar images (Rigo and Llasat, 2004). Unfortunately, from 2003 the network began to be either abandoned or transferred to other organisations and, as a result, has practically disappeared since 2015, with only a few 5-min rainfall stations still operative. The period analysed (1996–2015) included 44 stations, but after carrying out quality control (minimum length of 15 years, detection of data gaps and lack of continuity) this number was reduced to 30 (Fig. 2a).

The Júcar River Basin (CHJ in Fig. 1) has an extension of 22,261 km^2. The Júcar River is 497.5 km long and originates in the Iberian System at

1700 m altitude. It has a distinctly Mediterranean behaviour, characterised by a disproportion between ordinary and extraordinary water flows, with high rises in volume that cause catastrophic floods (Niclós Ferragut and Rodríguez Zurita, 2015). Like the CIC region, the coastal plains are crossed by torrential non-permanent streams around which intense urbanization has taken place. In the south of the region, the mountains almost reach the coastline (1558 m, Aitana) favouring heavy precipitation that can surpass 700 mm in 24 h. This was the case in November 1987 when 817 mm were recorded in 24 h (Millor Peñarrocha et al., 2002). In the case of the CHJ, 99 rainfall stations with 5-min rainfall rate series for the 1989–2015 period were selected from a total sample of 105 stations (Fig. 2b). Six stations were removed due to lack of homogeneity.

3. Methodology

3.1. Definition of indexes

In order to characterise the rainfall features of each region the following indexes, defined based on previous works (Llasat, 2001; Llasat et al., 2016), will be used hereinafter:

- Annual beta (β_A): The ratio between the total annual amount of precipitation (in mm) in which the intensity is greater or equal than 35 mm/h, and the total annual precipitation.

$$\beta_A = \frac{\sum PPT_A(I \geq 35\ mm/h)}{\sum PPT_{Atotal}}$$

- Mean annual beta ($\overline{\beta_A}$): The average of all the annual β_A's of the entire analysed period.
- Monthly beta (β_M): The ratio between the total monthly amount of precipitation (in mm) in which the intensity is greater or equal than 35 mm/h, and the total monthly precipitation.

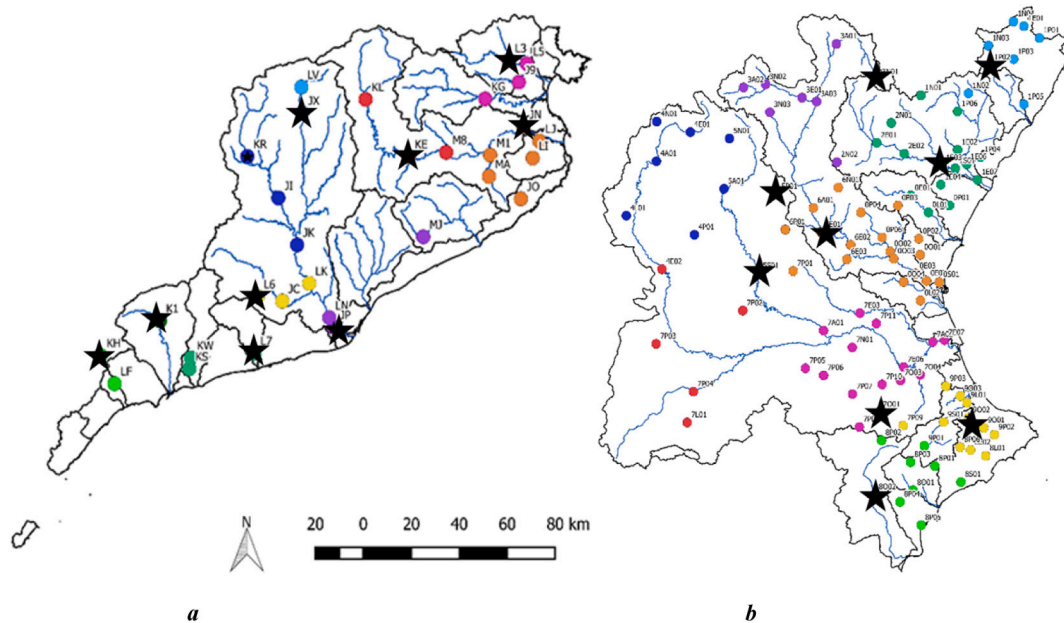$$\beta_M = \frac{\sum PPT_M(I_{5'} \geq 35\ mm/h)}{\sum PPT_{Mtotal}}$$

Fig. 3. Regions within the Internal Basins of Catalonia (a) and the Júcar Hydrographic Confederation (b) based on the convective features of precipitation. The stations used for this analysis are depicted with colour dots, depending on the cluster in question: pink (1), red (2), turquoise (3), light blue (4), dark blue (5), orange (6), purple (7), light green (8), yellow (9), and dark green (10). Representative stations are marked with a star.

- Mean monthly beta ($\overline{\beta_M}$): The average (by month) of all the monthly β_M for the entire period.
- Number of Convective Days (NCD): The number of days per month (NCD_M) or year (NCD_A) in which the 5-min intensity of 35 mm/h was exceeded at least once. These values are averaged by month/year and cover the entire period.
- Number of Convective Episodes (NCE): The number of episodes per month (NCE_M) or year (NCE_A) in which the 5-min intensity of 35 mm/h was exceeded at least once. Episodes are periods of continuous rainfall at a rainfall station separated by a gap of at least one hour. These values are also averaged by month/year and for the entire period.

Each episode can be characterised by a β_i value, in order to classify it depending on the convective contribution to total precipitation (very convective events, moderately convective events and, slightly convective events).

3.2. Rainfall regionalization and choice of example stations

The first step consists in the common regionalization of the CIC and the CHJ based on their rainfall features, following the methodology developed by Llasat et al. (2007), including the convective features of the precipitation, but updating to current rainfall networks and with the advantage of working with the Quantum GIS (Essen 2.14 version), which allows topographic factors to be included. The indicators chosen for each station were the geographic coordinates (UTM and altitude), average annual precipitation, average annual β value ($\overline{\beta_A}$), the maximum value of the monthly β average ($\overline{\beta_{M_{max}}}$), and the average annual number of convective days ($\overline{NCD_A}$). The cluster analysis was carried out using an R package that applies the K-means method based on Hartigan and Wong (1979). The number of clusters selected depends on the variance: an equilibrium between the maximum variance explained with the minimum number of clusters. A representative station was chosen for each cluster based on its quality (data series length and data continuity).

Table 1

Values for the most representative stations for each cluster within the CIC, showing: the code of the station (Co.) in Fig. 3a, the station name, the cluster number (C), the average annual precipitation in mm (AP), the average annual β ($\overline{\beta_A}$), the average annual number of rainfall episodes ($\overline{NE_A}$) and the average annual number of convective episodes ($\overline{NCE_A}$), and the average number of annual convective days ($\overline{NCD_A}$). The maximum value of monthly mean β ($\overline{\beta_{M_{max}}}$) and the month in which it is recorded ($M_{\beta M}$), the maximum monthly mean of convective days ($\overline{NCD_M}$) and the corresponding month (M_{CDM}) and the maximum monthly number of convective days (NCD_{max}).

| Co.	Name	C	AP	$\overline{\beta_A}$	$\overline{NE_A}$	$\overline{NCE_A}$	$\overline{NCD_A}$	$\overline{\beta_{M_{max}}}$	$M_{\beta M}$	$\overline{NCD_M}$	M_{CDM}	NCD_{max}
L3	Ponts Molins	1	672.1	0.12	173	8	7	0.25	9	1.2	9	7
KE	Sau	2	770.6	0.13	192	10	10	0.28	7	2.2	8	6
L7	Castellet i Gornal	3	515.0	0.16	150	8	7	0.28	9	1.8	9	4
JX	Baells	4	760.8	0.14	245	11	11	0.32	8	2.5	7	6
KR	Clariana Cardener	5	553.3	0.12	205	7	7	0.29	7	1.2	8	4
JN	Colomers	6	616.4	0.10	184	6	6	0.24	9	1.1	9	3
JP	St Joan Despí	7	505.3	0.12	145	7	6	0.25	7	1.3	9	4
KH	Cornudella Montsant	8	482.3	0.10	162	5	5	0.19	8	0.9	10	4
L6	St Quintí Mediona	9	513.4	0.14	149	7	7	0.32	8	1.5	9	4
K1	Montblanc	10	509.8	0.12	155	6	6	0.24	9	1.6	9	3
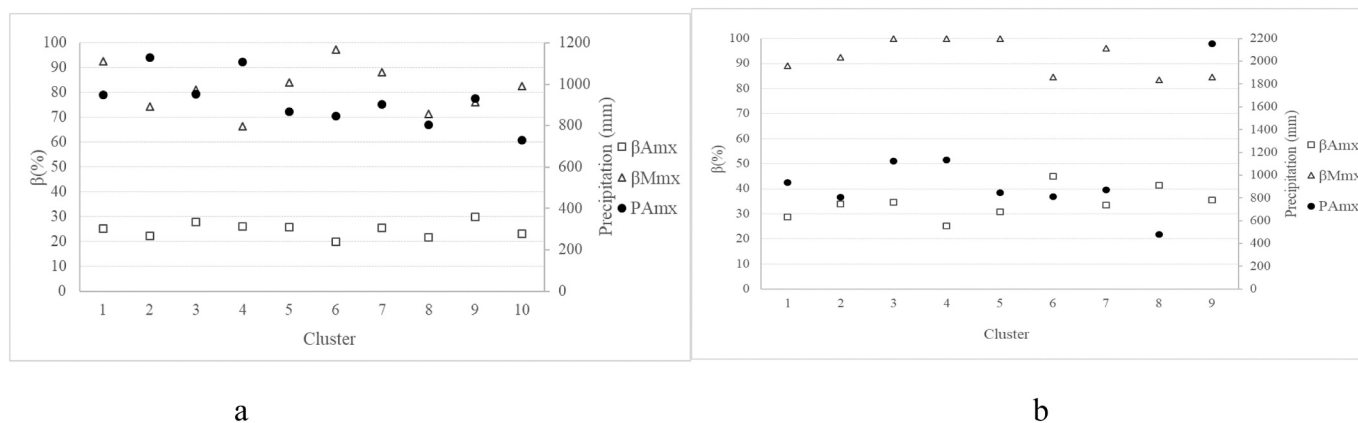
Fig. 4. Maximum values recorded in the representative station for each cluster within the CIC (a) and the CHJ (b), for the following variables: total precipitation recorded in a year (PAmx, mm), maximum annual β (βAmx, %), maximum monthly β (βMmx, %).
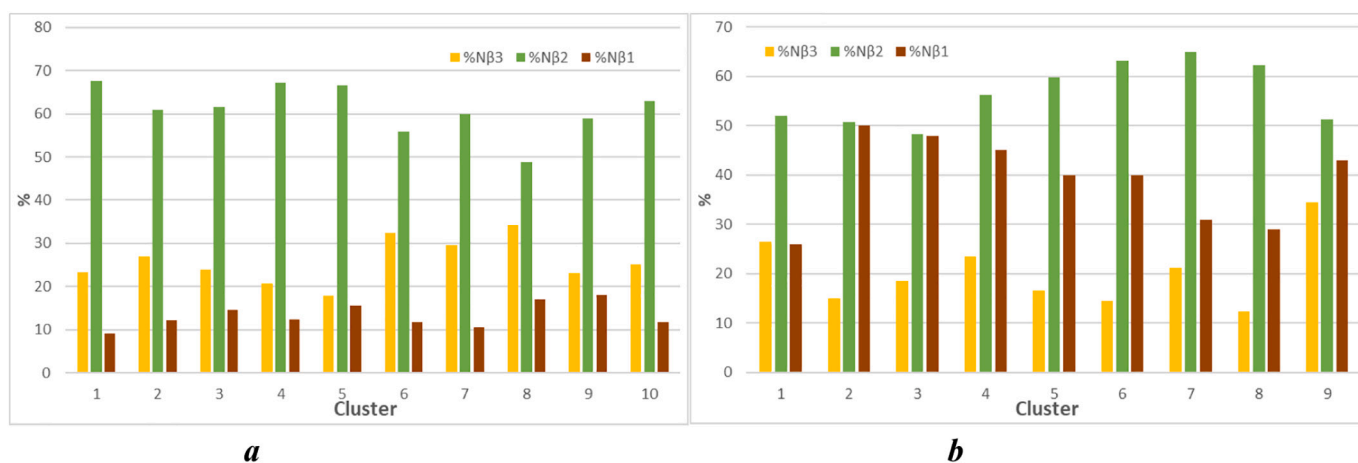

Fig. 5. Cluster distribution by categories, based on annual number of convective events for the CIC (a) and CHJ (b): very convective (β_1); moderately convective (β_2); slightly convective (β_3).

3.3. Trend analysis

The trend analysis was carried out by applying the Mann-Kendal non-parametric test using the R-package (Rai et al., 2013). Significance was distinguished for the thresholds of 90% and 95%. Trend analysis was applied to β, NCD and NCE, at an annual level.

4. Climatic features and regionalization

4.1. Spatial regionalization

The CIC and the CHJ are divided into 10 clusters, each shown in Fig. 3. The spatial dividing lines for the clusters were established keeping in mind the profiles of the basins. Table 1 describes the climatic characteristics in terms of annual rainfall and typology (based on β), as well as the convective nature on a monthly and episode-based scale, for each group of stations, and represented by the best quality station. Fig. 4 shows the maximum values for the different variables. Although the rainiest seasons are autumn and spring, the most convective season is summer, especially from July to September. More specifically, the average monthly β may reach 32% in August and 35% in September, for the CIC and the CHJ regions, respectively.

In the case of the CIC, the average annual precipitation shows values between 480 and 770 mm, with a gradient from south to north. The annual β parameter is very similar between the different regions, showing that, on average, between 10% and 16% of annual precipitation

has a 5-min rate intensity greater than 35 mm/h. However, this is generated by a very low percentage (between 3 and 6%) of convective events, in comparison with the total number of rainfall episodes. Clusters 2 (upper River Ter) and 4 (left basins upper River Llobregat), both placed near the Pyrenees Region, record the maximum annual precipitation; 1129.8 mm and 1109.5 mm, respectively. It is important to note that both clusters contain the most important dams within the CIC; Sau (River Ter, cluster 2) and La Baells (River Llobregat, cluster 4). The years with the maximum contribution from convective precipitation show β values greater than 22% for the entire region, with cluster 9 (middle section of the Llobregat river) recording the absolute maximum, with a β value near 30% (Fig. 4a). However, in clusters 4 and 9, and from a monthly point of view, an average of 32% of total precipitation exceeds s 35 mm/h in August. Also, β values exceed 66% in all clusters, and 97% in cluster 6,(Central Coast) for years that recorded the maximum percentage of convective precipitation. Finally, due to great interannual variability, the average monthly number of convective days is less than 3 days, although in some years it can increase up to 7 days. It is important to note that the most convective regions do not necessarily record the greatest total precipitation.

Fig. 5a shows the contribution of the different types of convective events for the CIC and the CHJ. The maximum relative contribution from slightly convective events in the CIC corresponds to cluster 8 (34.4%, south), which also records the minimum annual rainfall and the minimum β values (Table 1). The number of moderately convective episodes is highest in cluster 4, recording 153 episodes throughout the entire

Table 2

Values of the most representative stations for each cluster of the CHJ, showing: the code of the station (Co.) in Fig. 3, the station name, the cluster number (C), the average annual precipitation in mm (AP), the average annual β ($\overline{\beta_A}$), the average annual number of pluviometric episodes ($\overline{NE_A}$) and the average annual number of convective episodes ($\overline{NCE_A}$), the average number of annual convective days ($\overline{NCD_A}$), the maximum value of monthly mean β ($\overline{\beta_{M_{max}}}$) and the month in which it is recorded ($M_{\beta M}$), the maximum monthly mean of convective days ($\overline{NCD_M}$) and the corresponding month (M_{CDM}), and the maximum monthly number of convective days (NCD_{max}).

Code	Name	C	AP	$\overline{\beta_A}$	$\overline{NE_A}$	$\overline{NCE_A}$	$\overline{NCD_A}$	$\overline{\beta_{M_{max}}}$	$M_{\beta M}$	$\overline{NCD_M}$	M_{CDM}	NCD_{max}
7O01	River Cañoles	1	596.1	0.10	148	5	5	0.26	9	1.33	9	5
5S01	Contreras (pluviometer)	2	455.4	0.12	172	5	5	0.22	9	1.07	9	4
1E03	Ribesalbes (dam)	3	477.6	0.13	160	5	5	0.30	9	1.44	9	6
1P02	Catí (pluviometer)	4	694.5	0.14	173	8	8	0.31	8	1.63	9	6
5P01	Landete (pluviometer)	5	516.2	0.11	205	6	6	0.24	8	1.22	9	5
6E01	Benagéber (dam)	6	525.4	0.13	153	7	6	0.27	8	1.15	9	5
3 N01	Gúdar (pluviometer)	7	589.4	0.13	209	8	8	0.32	8	2.04	8	5
8O02	Elda	8	300.5	0.14	116	4	4	0.22	9	0.82	9	4
9O02	Rambla Gallinera	9	1094.1	0.18	164	11	10	0.35	9	2.19	9	8

period for the northern coastal area. Also, the maximum relative contribution from moderately convective events corresponds to cluster 1 (67.5%) and cluster 4 (67.1%), both located in the Pre-Pyrenees range in the northern part of the region. The Maresme and Barcelonès counties, on the central coast, where more than 50% of the population lives, record nearly 5% of convective events, with a distribution of 29.5% of very convective events, 59.8% of moderately convective events, and 10.6% of slightly convective events. These counties include part of the Coastal range, which shows that although proximity to the Pyrenees favours total annual precipitation, the main relative convective contribution is recorded near the Pre-Coastal range. This may be explained by the fact that most of the rivers with catchments below 1000 km², and non-permanent and torrential streams have their sources in the Pre-Coastal and Coastal ranges, respectively. These features justify the high frequency of flash floods caused by this type of precipitation which, on some occasions, can have catastrophic consequences, like in the case of September 1962, June 2000, or October 2018, with 815, 5, and 7 casualties, respectively.

From all these observations, it can be deduced that the areas with the highest rainfall, located on the Pyrenees foothills, have the greatest ratio of moderately convective and slightly convective episodes. In the regions where very convective episodes predominate, like in the Coastal mountain range, monthly and annual average precipitation is not so high. This indicates that they are due to different atmospheric processes.

In the case of the CHJ, 9 clusters were selected (Fig. 3b). The difference in annual rainfall between clusters is greater than for the CIC. More specifically, cluster 9 (known as "Marina Alta"), near the coast and Coastal mountain range, records average annual precipitation levels close to 1100 mm/year, while cluster 8 (known as "Marina Baja"), adjacent to the previous one, records close to 300 mm/year (Table 2). The average number of annual rainfall episodes and those of a convective character are within the same range as for the CIC, with maximum values of 209 and 11, respectively. In addition, it is clear from the comparison of the two regions that the most convective season in the CHJ is in the months of August and September, which suggests a later convective season.

The contribution of 5-min rate precipitation above 35 mm/h to total precipitation (β) in the CHJ presents values within the range of those obtained for the CIC. However, station 9002 (cluster 9) at the foot of the Aitana mountain range and near the coast, stands out among the rest of the stations. In this case, 6.7% of the station's annual rainfall episodes are convective, contributing 18% to annual average precipitation. In the Aitana region, September is the most convective month, producing 35% of total monthly precipitation. In the same station, there is an absolute maximum of 2156.39 mm for annual precipitation (double the annual average), and a maximum monthly β of 85%. The contribution of the most convective summers in the CHJ was significantly higher than those recorded in the CIC. More specifically, values of β higher than 83% were recorded for the entire CHJ region, reaching 100% for clusters 3, 4, and

5 (Fig. 4b). This is consistent with the heavy rainfall recorded in the area, which may accumulate more than 500 mm in 24 h and, on some occasions, even reach 1000 mm.

Fig. 5b shows that cluster 9 in the CHJ records 302 convective events along the entire period, while region 8 records the minimum number, with 114 convective events. Of these episodes, moderately convective events comprise between 48% and 65%, while slightly convective events represent between 12% and 26%. The most important feature is the greater contribution from very convective events, which exceeds 10% across all the clusters, and reaches 34% in clusters 2 and 3. This contribution is considerably higher than the one produced by events of this type registered in the CIC, which does not exceed 20%. In both regions, the most common pattern for episodes is moderately convective events, either as a result of more continuous rainfall of moderate intensity, or by registering peaks of very strong intensity embedded in relatively weak rain. As usual, the region with the highest contribution of convective events, as well as total precipitation, does not record the maximum contribution from very convective events, which usually have a short duration.

The differences between the CHJ and the CIC corroborates the decisive role played by orography regarding the spatial structure of precipitation over land. This is not only due to elevation, which can trigger convection, but is also due to the orientation of the mountain ranges with respect to impinging air from the Mediterranean Sea and their proximity to the coastline (Llasat and Puigcerver, 1992; Romero et al., 1997). These factors justify the strong precipitation recorded in the foothills of the Aitana mountain range (CHJ), when the moist eastern and northeastern flow, usually produced by the circulation of the Algerian low created in the northern lee of the Atlas mountain, impinges perpendicularly to it (Romero et al., 1997). In the case of Catalonia and the north of the CHJ, although there is also a Coastal range, its altitude does not exceed 600 m. This range triggers local convection, mainly when it impinges over a moist and warm flow from the southeast. This flow usually results from a mesoscale low between Catalonia and the Balearic Islands, which in some occasions has also previously travelled over the Aitana region (Llasat, 2009). In their objective classification of precipitation patterns, Romero et al. (1999) consider that southern Valencia, along with Murcia (to its south), configure a pattern characterised by the most abundant rainfall in the Spanish Mediterranean region, with a maximum surrounding the Aitana mountain range, while the general area of Valencia and southern Catalonia shows an elongated shape parallel to the coastal mountains. In line with these authors, these patterns are slightly modified when they refer to torrential rainfall, which can explain our findings. In this case, the maximum over the Aitana mountain range is the most significant (long-lasting moderate convective events), and there is a marked suppressing gradient from the coast inland that characterises Catalonia (local and short very convective events), although the proximity of the Pyrenees creates a maximum inland in the northern part of the region.
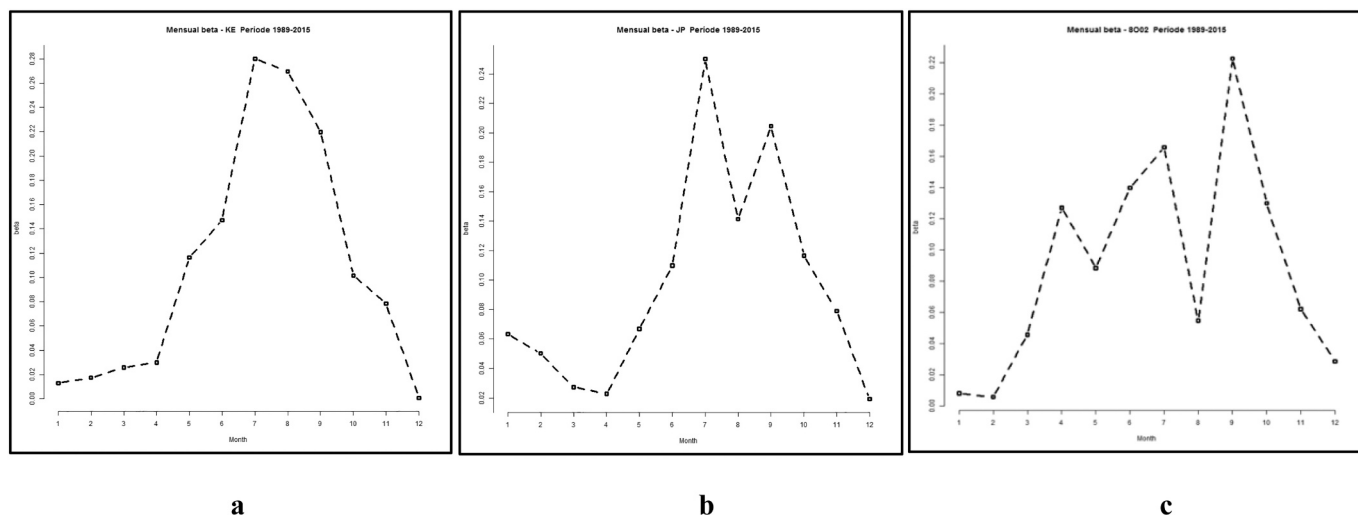
Fig. 6. Example of the monthly β distribution along the year: (a) Unimodal; (b) Bimodal; c) Trimodal.

Table 3
Pattern of β monthly distribution for each selected station, and the months corresponding to each peak or peaks.

CIC	L3	KE	L7	JX	KR	JN	JP	KH	L6	K1
Mode	1	1	1	1	1	1	2	2	1	1
Month	9	7	9	8	7	9	7;9	6;8	8	9
CHJ	7O01	5S01	1E03	1P02	5P01	6E01	3 N01	8O02	9O02	
Mode	1	2	2	1	1	1	1	3	1	
Month	9	6;9	5;9	8	8	8	8	4;7;9	9	

Table 4
Annual trends of precipitation and convective parameters expressed in change/decade for the 1996–2015 period in the CIC and the 1989–2015 period in the CHJ. The numbers in bold mean that the trend is significant at 90%, while an asterisk indicates a significance of 95%, following the Mann Kendall analysis. The columns are: cluster number (**C**), annual precipitation in mm/decade (**AP**), annual β (**$β_A$**), number of annual convective days (**N_{CDA}**), and annual number of convective episodes (**N_{ACE}**).

Code	C	AP	$β_A$	N_{CDA}	N_{CEA}
KE	2	9.6	0.005	0.481	0.609
L7	3	−32.3	0.007	0.654	0.068
JX	4	−97.8	0.021	−0.677	−0.195
KR	5	−31.1	0.032	0.647	1.256
JP	7	−89.5	−0.011	−0.429	−0.135
L6	9	**−160.0**	0.023	−0.030	−0.015
K1	10	−28.6	0.004	0.662	0.940
7O01	1	33.6	**0.035***	**1.716***	**1.740***
5S01	2	−12.4	−0.015	**−1.691***	**−1.795***
1E03	3	−6.1	**0.044***	**1.368**	**1.532**
1P02	4	55.8	**0.026***	0.525	0.525
5P01	5	79.7	0.031	**1.624***	**1.996***
6E01	6	21.5	**0.050***	0.995	1.661
3N01	7	**83.1***	0.028	**1.929***	**1.972***
8O02	8	14.3	−0.034	**−1.282***	**−1.233***
9O02	9	49.9	**0.035**	1.148	1.386

4.2. Monthly climatology

In response to the number and distribution of the maximum values of monthly β over an average year, there are three behaviour patterns: unimodal, bimodal, and trimodal (Fig. 6). The unimodal pattern is the most frequent, is characterised by a maximum in the summer (JAS), and has been found in 73% of the stations in both regions. In 27% of cases, the maximum corresponded to July, while August registered 23% and September 50%. On the other hand, the bimodal pattern is characterised by a very marked minimum in the middle of summer, surrounded by two

maximums that are also recorded in this season. It is more common in stations located inland, far from the mountains, which hardly register precipitation in August. This pattern was only identified in 21% of the stations. Regarding the trimodal pattern, it is only registered in the Aitana mountain range and may be a consequence of the orographic effect that triggers convection when a cold front arrives from the west (usually in spring), or moist and warm air arrives from the east (Table 3). This differentiated behaviour is closely related to the complicated role that orography plays in Spain, as demonstrated by Álvarez-Rodríguez et al. (2017) from a climatic point of view. In effect, del Moral et al. (2020) showed the triple role of mountains, which can trigger convection, and help the formation of an instability line over which thunderstorms grow, and make the movement of storm cells more difficult.

5. Trend analysis

Table 4 shows the trends for the 1996–2015 period, for both the CIC and CHJ stations that cover the complete series. In this case, all the stations with a significant trend of β (44% of the total number of stations) show positive values. In the case of NCD and NCE, the trends are significant for only 37.5% of the stations, and in this case, 67% have positive values. There is a notable difference in terms of the significance of trends between one region and another. While in the case of the CIC the trends are, in general, not significant, in the CHJ they are much more marked. For instance, in the case of the CHJ, there is a notable increase in the annual β value that reaches 5%/10y (6E01). This increase in convective precipitation would be distributed across a greater number of episodes and a greater number of days, with significant trends in these variables that reach almost 20 days/century and 20 convective episodes/century, respectively. Only two stations in the CHJ would present significant negative trends for NCE and NCD. These two stations show a different pattern of β monthly distribution: maximum in late spring and late summer (5S01) and a trimodal pattern (8O02), that corroborates the different atmospheric processes associated with the precipitation in
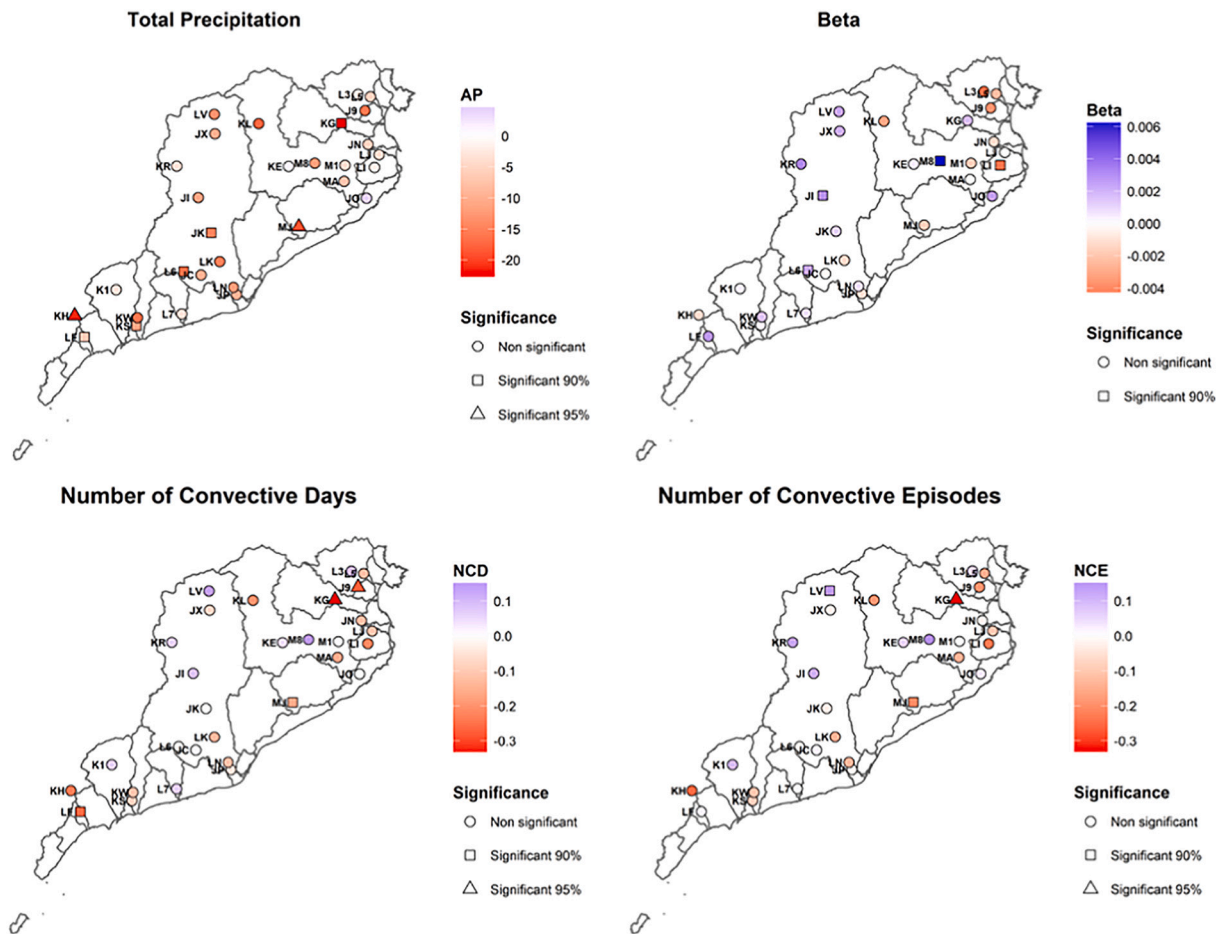
Total Precipitation

Beta

Number of Convective Days

Number of Convective Episodes

Fig. 7. Spatial distribution of trends found in the CIC and corresponding to: annual precipitation, annual β, annual number of convective days and convective episodes. Significance was obtained following the Mann-Kendall test.

regions 2 (far from the coast and Coastal and Pre-Coastal ranges) and 8 (leeward of the Aitana mountain range with respect to Mediterranean air advection).

In the case of the CIC, annual β trends also point to an increase while annual precipitation decreases, which indicates an increase in convective contribution. This is particularly relevant in the Llobregat basin (represented by L6), where the number of convective days and convective events also decreases, pointing to an increase in the torrentiality of the episodes (precipitation concentrated in fewer events). These results are consistent with the hypothesis of the (IPCC, 2014) and (IPCC, 2018) which points to an increase in heavy rainfall.

Fig. 7 shows a general decrease in precipitation over the 20 year period in the CIC. This is a notable result if we compare it with the Third Report on Climate Change in Catalonia (Martín Vide, 2016), in which a common trend had not been found when the series ended in 2011, but it is more coherent with climate change scenarios. Despite this negative trend, convective precipitation has increased its contribution throughout the year across the entire region except for the most north-eastern part, where there is a decrease in the value of all the variables. The increase in convective precipitation shows two patterns; the first one points to an increase in the number of convective episodes and days and characterises the inland part of the CIC (mainly the Llobregat Basin). On the other hand, on the coast, the negative trend of convective episodes and days points to an increase in more torrential events, probably produced by thunderstorms, and usually more dangerous due to their high intensities. Seasonal analysis shows that this behaviour is particularly significant in the summer season (JAS).

Fig. 8 shows the spatial distribution of the trend for the different variables analysed over the 1989–2015 period in the CHJ. In this case, the period is longer, so the results should be more robust. In general, there is a decrease in annual rainfall on the coast, except for clusters 8 and 9 (Marina Alta and Marina Baja) located in the region of the Aitana mountain range. On the other hand, inland and in the Aitana mountain range, numerous stations experienced an increase in precipitation, a trend that is not observed in the CIC. Both β and the number of days and convective episodes increased across most of the region. In this case the increase in the torrentiality of the episodes is not as marked as in the CIC, except for the coast, given the decrease in annual precipitation. In addition, as Table 4 corroborates, the positive trend of convective precipitation is much more significant than in the CIC, probably because of the greater length of the series and the increase in total precipitation.

6. Conclusions and discussion

In the present paper, we have conducted a characterisation and trend analysis of convective precipitation for a large area of the Mediterranean region in Spain. Although the total area is less than 40,000 km², it represents the degree of spatial and temporal variability of heavy precipitation events quite well. It also shows the strong role played by the orography surrounding a warm sea, which characterises the Mediterranean region, giving rise to high-impact atmospheric processes, as analysed in depth in Michaelides et al. (2018).

The region of study is made up of two hydrographic basins, the Internal Basins of Catalonia, managed by the Water Catalan Agency, (the CIC), and the Júcar, managed by the Júcar Hydrographic Confederation, (the CHJ), with a total of 148 automatic rain gauges, that, after quality
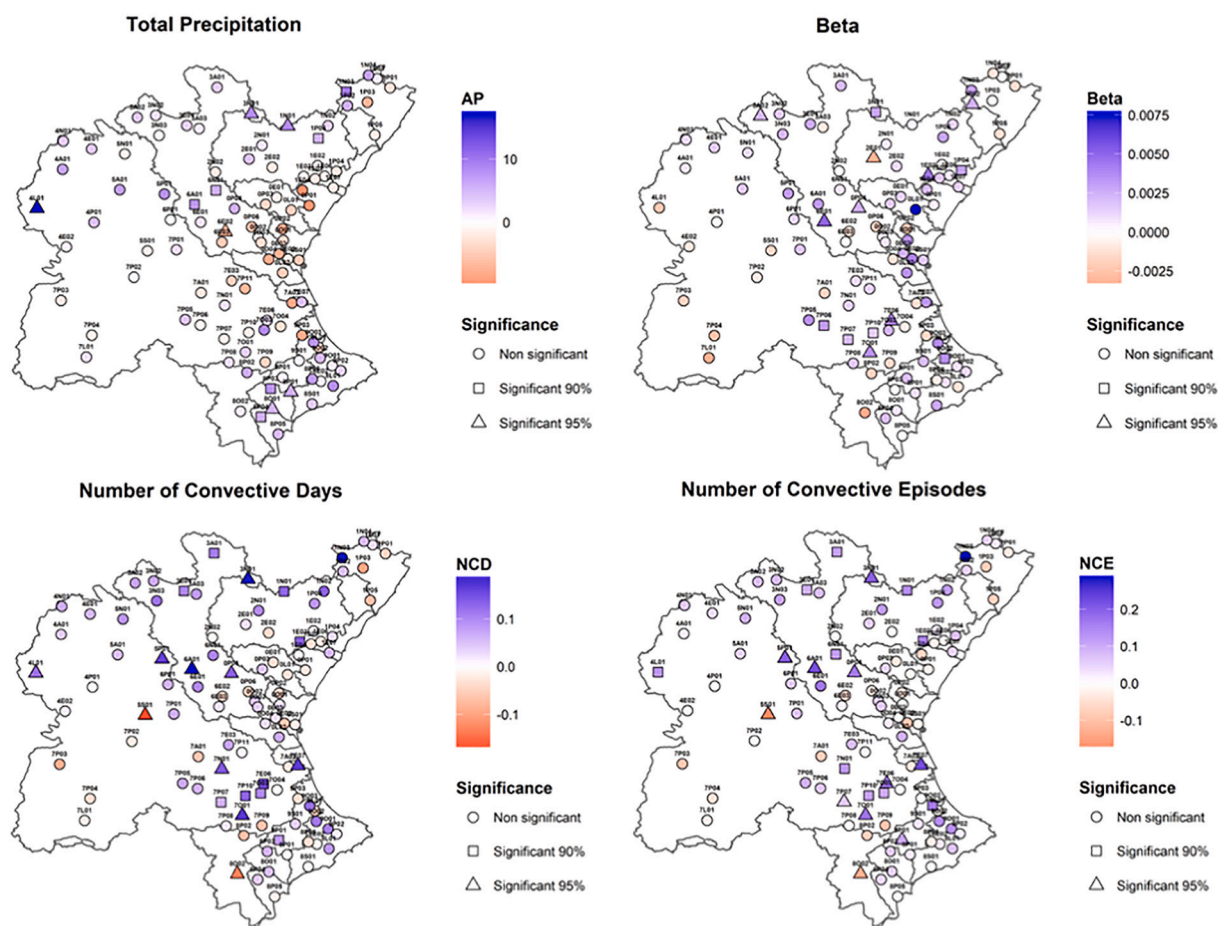
Fig. 8. Spatial distribution of the trends found in the CHJ and corresponding to: annual precipitation (**AP**), annual β, annual number of convective days (**NCD**) and convective episodes (**NCE**). Significance has been obtained following the Mann-Kendall test.

control, provided 129 series of 5-min rainfall rates. They were clustered in 19 homogeneous regions according to total precipitation and convective precipitation features. Each region was represented by the best rainfall station. The total average annual amount of precipitation is between 455 mm and 1094 mm in the CHJ, and 482 mm and 741 mm in the CIC. In the latter case, the area with the highest annual precipitation is favoured by the effect of the eastern part of the Pre-Pyrenees mountain ranges, where there is a convergence zone for convection (Del Moral et al., 2016). A similar situation occurs in the Aitana mountain range, in the CHJ, where 18% of the annual precipitation has a 5-min intensity rate is greater than 35 mm/h, which is the threshold used to define convective precipitation, reaching 35% in September. However, the role of the Coastal mountain range is very important, since it encourages the most violent precipitation phenomena, with high intensities throughout the entire episode, usually causing sudden surface water floods and flash floods (Llasat et al., 2016; Cortès et al., 2019). In particular, it is no surprise that in some summer months more than 90% of the events are convective. A comparison between both regions shows that torrentiality is greater in the CHJ, with some months in which β is equal to 100%,and has a higher relative and absolute number of very convective events. This can be explained not only by the orography and proximity to the sea, but also due to the major frequency of the meteorological and maritime factors that favour heavy rainfalls in the case of the CHJ. Although the presence of a surface low is often associated with heavy rainfall in both regions (Romero et al., 1999; Jansà et al., 2014), Sea Surface Temperature (SST) is higher in the southern part of the western Mediterranean, and it plays a decisive role in the development of convective precipitation (Llasat and Puigcerver, 1997).

In summary, the study of precipitation from 5-min series in the east

of the Iberian Peninsula shows that the contribution of convective precipitation is highest in late summer (mainly August or September, when it can reach 100%). On average, between 10% and 20% of annual precipitation is convective, although some years this can be as high as 30%. This precipitation is caused by less than 5% of annual rain episodes (it only exceeds 6% in the Aitana mountain range), which corroborates that it is associated to heavy rains. Orography (both in terms of height and orientation) and the SST play a very important role. Greater height near the sea, favourable orientation to force ascent and higher SST favour convection in the south of the analysed region, as well as episodes of torrential rains in which nearly 100% of the precipitation can exceed 35 mm in 5 min. While, on an annual average, less than 20% of the episodes in the CIC are highly convective (β > 75%), in the CHJ it exceeds 30%.

The second conclusion refers to the lack of a common trend towards drier conditions for the CIC and the CHJ. A negative trend characterises a large part of the CIC, and it is most remarkable in the northeastern region. On the other hand, for the analysed period, there was a positive trend in the CHJ. These results are consistent with the climatic projections for the 2011–2040 period proposed by CEDEX (2011), based on the A2 scenario, and by Turco et al. (2017), after applying a statistical downscaling over seven members of the regional climate models produced by the ENSEMBLES project. These authors show that the difference between both regions is mainly due to the contributions in winter and spring.

The third conclusion points to an increase in convective precipitation, mainly in the coastal section of our region of study. Although some studies have found an increase in heavy precipitation events (i.e. de Lima et al., 2014 for Portugal; Tramblay and Somot, 2018, for future scenarios in the northern part of the Mediterranean basin), no significant

trend has been found for the maximum daily precipitation in the eastern region of Spain, neither at present (Turco and Llasat, 2011) nor for the near future (Turco et al., 2017). The increase in convective precipitation might not be detected in the maximum daily precipitation, since it is usually related to short episodes in which the precipitation amount is less than 100 mm. In this sense, Cortès et al. (2019) selected the threshold of 40 mm as the minimum precipitation for flash floods in the study region, showing that the precipitation caused by these events will increase in the future.

The fourth conclusion emphasises that this increase in convective precipitation is concentrated in fewer episodes, which implies greater torrentiality for precipitation. Similar results were obtained by Burić et al. (2015), showing that in Montenegro the number of days with precipitation decreased, while rainfall intensity increased.

These results could be related to a present and future increase in local flash floods in the northwestern part of the Mediterranean basin (Llasat et al., 2013; Cramer et al., 2018), although it is difficult to separate the hazard (precipitation driver) from exposure and vulnerability factors (ill-conceived stormwater management systems, sealed urban surfaces, occupation of flood-prone regions, etc.). Following the analysis of more than 500 years of data covering all of Europe, Blöschl et al. (2020) has shown that the flood-rich period starting in 1990 is the third largest in a spatio-temporal sense, and that this situation is linked to a change in the processes that cause the floods, as the other flood-rich periods occurred in abnormally cold situations. Floods in Central Europe have increased mainly in the summer, and the authors consider that thermodynamic conditions play a major role at present, favouring the feeding of convective processes. Although they have only taken into account river floods and not flash floods in ungauged catchments (those included in the papers by Llasat et al., 2013 and Cortès et al., 2019), they also find an increase in the Mediterranean that is associated with an increase in evaporation and convective activity. The present paper is good proof of this increase in convective precipitation.

The most remarkable conclusion of this work is the increase in convective precipitation that is occurring in most of the Mediterranean region of Spain, concentrated in fewer events. Until now, the trends observed in maximum daily rainfall were not in accordance with the expected impact of climate change as a result of the increase in humidity and instability in the atmosphere. However, the results of this work show that the trends are in accordance with this impact when working on a sub-daily temporal scale. The increase in flash and local floods in other Mediterranean regions points to a possible generalisation of the increase in convective precipitation.

Author statement

M.C. Llasat designed the study, provided guidance for the analyses, wrote the paper, acquired funding for the investigation and was responsible of projects administration. M. Cortès and A. del Moral were the responsible of data curation, formal analysis, figures design and software. T. Rigo contributed in the supervision and validation. All authors contributed to framing, revising and editing the paper.

Declaration of Competing Interest

The authors declare that they have no known competing financial interests or personal relationships that could have appeared to influence the work reported in this paper.

Acknowledgements

References

Adelfio, G., Chiodi, M., D'Alessandro, A., Luzio, D., 2011. FPCA algorithm for waveform clustering. J. Commun. Comput. 8 (6), 494–502.

Alexander, L.V., Zhang, X., Peterson, T.C., Caesar, J., Gleason, B., Tank, K., Haylock, M., et al., 2006. Global observed changes in daily climate extremes of temperature and precipitation. J. Geophys. Res.-Atmos. 111 (D5) https://doi.org/10.1029/2005JD006290.

Álvarez-Rodríguez, J., Llasat, M.C., Estrela, T., 2017. Analysis of geographic and orographic influence in Spanish monthly precipitation. Int. J. Climatol. https://doi.org/10.1002/joc.5007.

Berg, P., Haerter, J.O., 2013. Unexpected increase in precipitation intensity with temperature—a result of mixing precipitation types? Atmos. Res. 119, 56–61.

Berg, P., Moseley, C., Haerter, J.O., 2013. Strong increases in convective precipitation in response to higher temperatures. Nat. Geosci. 6, 181–185.

Blöschl, G., Kiss, A., Viglione, A., et al., 2020. Current flood-rich period is exceptional compared to the past 500 years in Europe. Nature 583, 560–566. https://doi.org/10.1038/s41586-020-2478-3.

Burić, D., Luković, J., Bajat, B., Kilibarda, M., Živković, N., 2015. Recent trends in daily rainfall extremes over Montenegro (1951–2010). Nat. Hazards Earth Syst. Sci. 15, 2069–2077. https://doi.org/10.5194/nhess-15-2069-2015.

CEDEX, 2011. Evaluación del impacto del cambio climático en los recursos hídricos en régimen natural. In: Encomienda de Gestión de la Dirección General del Agua (MARM) al CEDEX Para el Estudio del Cambio Climático en los Recursos Hídricos y las Masas de Agua. Centro de Estudios y Experimentación de Obras Públicas, 269 pp. Madrid.

Chou, C., Chen, C.-A., Tan, P.-H., Chen, K.T., 2012. Mechanisms for global warming impacts on precipitation frequency and intensity. J. Clim. 25, 3291–3306.

Cortès, M., Turco, M., Ward, Ph., Sánchez-Espigares, J., Alfieri, L., Llasat, M.C., 2019. Changes in flood damage with global warming in the east coast of Spain. Nat. Hazards Earth Syst. Sci. 19, 2855–2877. https://doi.org/10.5194/nhess-2019-253.

Cramer, W., Guiot, J., Fader, M., Garrabou, J., Gattuso, J.-P., Iglesias, A., Lange, M.A., Lionello, P., Llasat, M.C., Paz, S., Peñuelas, J., Snoussi, M., Toreti, A., Tsimplis, M.N., Xoplaki, E., 2018. Climate change and interconnected risks to sustainable development in the Mediterranean. Nat. Clim. Chang. 8, 972–980. https://doi.org/10.1038/s41558-018-0299-2.

de Leon, D.C., et al., 2016. The Convective Precipitation Experiment (COPE): investigating the origins of heavy precipitation in the southwestern United Kingdom. Bull. Am. Meteorol. Soc. 97 (6), 1003–1020.

de Lima, M.I.P., Santo, F.E., Ramos, A.M., Trigo, R.M., 2014. Trends and correlations in annual extreme precipitation indices for mainland Portugal, 1941–2007. Theor. Appl. Climatol. 119 (1–2), 55–75. https://doi.org/10.1007/s00704-013-1079-6.

Del Moral, A., Llasat, M.C., Rigo, T., 2016. Identification of anomalous motion of thunderstorms using daily rainfall fields. Atmos. Res. 185, 92–100. https://doi.org/10.1016/j.atmosres.2016.11.001.

Del Moral, A., Llasat, M.C., Rigo, T., 2020. Connecting flash flood events with radar-derived convective storm characteristics on the Northwestern Mediterranean coast: knowing the present for better future scenarios adaptation. Atmos. Res. 238, 104863. https://doi.org/10.1016/j.atmosres.2020.104863, 1 July 2020.

Dutton, E.J., Dougherty, H.T., 1979. Year-to-year variability of rainfall for microwave applications in the U.S.A. IEEE Trans. Comm. 829–832. COM-27 5.

Francipane, A., Sottile, G., Adelfio, G., Noto, L.V., 2020. Convective and Stratiform Precipitation: A PCA-Based Clustering Algorithm for their Identification. EGU2020-18518. https://doi.org/10.5194/egusphere-egu2020-18518.

Hartigan, J.A., Wong, M.A., 1979. Algorithm AS 136: a K-means clustering algorithm. Appl. Stat. 28, 100–108. https://doi.org/10.2307/2346830.

Houze, R., 1977. Stratiform precipitation in regions of convection: a meteorological paradox? Bull. Am. Meteorol. Soc. 78, 2179–2197.

Houze Jr., R.A., Wilton, D.C., Smull, B.F., 2007. Monsoon convection in the Himalayan region as seen by the TRMM Precipitation Radar. Q. J. R. Meteorol. Soc. 133, 627,1389–1411.

IPCC, 2014. AR5 Climate change 2014: impacts, adaptation, and vulnerability. IPCC Working Group II contribution to the fifth assessment report of the Intergovernmental Panel on Climate Change. Cambridge Univ. Press, England.

IPCC, 2018. Special Report on Global Warming of 1.5 °C of the Intergovernmental Panel on Climate Change. Cambridge Univ. Press, England.

Jansà, A., Alpert, P., Arbogast, P., Buzzi, A., Ivancan-Picek, B., Kotroni, V., Llasat, M.C., Ramis, C., Richard, E., Romero, R., Speranza, A., 2014. MEDEX: a general overview. Nat. Hazards Earth Syst. Sci. 14 https://doi.org/10.5194/nhess-14-1965-2014, 1965–198.

Lenderink, G., van Meijgaard, E., 2008. Increase in hourly precipitation extremes beyond expectations from temperature changes. Nat. Geosci. 1, 511–514.

Lepore, C., Veneziano, D., Molini, A., 2015. Temperature and CAPE dependence on rainfall extremes in the eastern United States. Geophys. Res. Lett. 42, 74–83.

Llasat, M.C., 2001. An objective classification of rainfall events on the basis of their convective features. Application to rainfall intensity in the north-east of Spain. Int. J. Climatol. 21 (11), 1385–1400.

Llasat, M.C., 2009. Chapter 18: Storms and floods. In: The Physical Geography of the Mediterranean Basin. Edited by Jamie Woodward. Published by Oxford University Press, pp. 504–531. ISBN: 978–0–19-926803-0.

Llasat, M.C., Puigcerver, M., 1985. Un intento de aplicación a la Península Ibérica de un modelo empírico de precipitación. Revista de Geofísica 41, 135–144.

Llasat, M.C., Puigcerver, Y.M., 1992. Pluies extremes en Catalogne: influence orographique et caractéristiques synoptiques. Hydrol. Cont. 2, 99–115 (Ed. Orstom). ISSN: 0246-1528. Paris, Francia. 1992.

Llasat, M.C., Puigcerver, M., 1997. Total rainfall and convective rainfall in Catalonia, Spain. Int. J. Climatol. 17, 1683–1695.

Llasat, M.C., Rigo, T., Barriendos, M., 2003. The "Montserrat-2000" flash-flood event: a comparison with the floods that have occurred in the North-Eastern Iberian Peninsula since the 14th century. Int. J. Climatol. 23, 453–469.

Llasat, M.C., Ceperuelo, M., Rigo, T., 2007. Rainfall regionalization on the basis of the precipitation convective features using a raingauge network and weather radar observations. Atmos. Res. 83, 415–426.

Llasat, M.C., Llasat-Botija, M., Petrucci, O., Pasqua, A.A., Rosselló, J., Vinet, F., Boissier, L., 2013. Towards a database on societal impact of Mediterranean floods in the framework of the HYMEX project. Nat. Hazards Earth Syst. Sci. 13 (1–14) https://doi.org/10.5194/nhess-13-1-2013 www.nat-hazards-earth-syst-sci.net/13/1/2013/.

Llasat, M.C., Marcos, R., Turco, M., Gilabert, J., Llasat-Botija, M., 2016. Flash floods trends versus convective precipitation in a Mediterranean region. J. Hydrol. 541, 24–37. https://doi.org/10.1016/j.jhydrol.2016.05.040 0022-1694.

Martín Vide, J., 2016. Tercer Informe sobre el canvi climàtic a Catalunya. Barcelona. In: Generalitat de Catalunya i Institut d`Estudis Catalans. ISBN 9788499653174 (IEC). – ISBN 9788439394488 (Generalitat de Catalunya) (611 pp) (coord.).

Michaelides, S., Karacostas, T., Sánchez, J.L., Retalis, A., Pytharoulis, I., Homar, V., Romero, R., Zanis, P., Giannakopoulos, C., Bühl, J., Ansmanng, A., Merino, A., Melcón, P., Lagouvardos, K., Kotroni, V., Bruggeman, A., López-Moreno, J.I., Bertheti, C., Katragkou, E., Tymvios, F., Hadjimitsis, D.G., Mamouri, R., Nisantzi, A., 2018. Reviews and perspectives of high impact atmospheric processes in the Mediterranean. Atmos. Res. 208, 4–44. https://doi.org/10.1016/j.atmosres.2017.11.022.

Millor Peñarrocha, D., Estrela, M.J., Millán, M., 2002. Classification of daily rainfall patterns in a Mediterranean area with extreme intensity levels: the Valencia region. Int. J. Climatol. 22 (6), 677–695.

Niclós Ferragut, J., Rodríguez Zurita, M., 2015. Water Management and Early Warning Tools at SAIH-Júcar 19th International Congress on Project Management and Engineering. Granada, 15-17th July 2015.

Puigcerver, M., Alonso, S., Lorente, J., Llasat, M.C., Redaño, A., Burgeño, A., Vilar, E., 1986. Preliminary aspects on rainfall rates in the north east of Spain. Theor. Appl. Climatol. 37, 97–109.

Rai, R.K., Upadhyay, A., Ojha, C.S.P., Lye, L.M., 2013. Statistical analysis of hydro-climatic variables (ed. 2013). In: Surampalli, R.Y., Zhang, T.C., Ojha, C.S.P., Gurjar, B.R., Tyagi, R.D., Kao, C.M. (Eds.), Climate Change Modelling, Mitigation, and Adaptation. ASCE, Reston, VA. https://doi.org/10.1061/9780784412718.

Ramis, C., Llasat, M.C., Genovés, A., Jansà, A., 1994. The October-87 floods in Catalonia. Synoptic and Mesoscale Mechanisms. Meteorological Applications 1, 337-350. (Royal Meteorological Society). (ISSN: 1350-4827).

Rice, P.L., Holmberg, N.R., 1973. Cumulative time statistics of surface-point rainfall rates. IEEE Trans. Comm. COM-21 (10), 1131–1136.

Rigo, T., Llasat, M.C., 2004. A methodology for the classification of convective structures using meteorological radar: application to heavy rainfall events on the mediterranean coast of the iberian peninsula. Nat. Hazards Earth Syst. Sci. 4, 59–68.

Rigo, T., Berenguer, M., Llasat, M.C., 2019. An improved analysis of mesoscale convective systems in the Western Mediterranean using weather radar. Atmos. Res. 227, 146–157. https://doi.org/10.1016/j.atmosres.2019.05.001. October 2019.

Romero, R., Ramis, C., Alonso, S., 1997. Numerical simulation of an extreme rainfall event in Catalonia: role of orography and evaporation from the sea. Quart. J. R. Meteorol. Soc. 123, 537–559.

Romero, R., Ramis, C., Guijarro, J.A., 1999. Daily rainfall patterns in the Spanish Mediterranean area: an objective classification. Int. J. Climatol. 19, 95–112.

Schumacher, C., Houze Jr., R.A., 2003. Stratiform rain in the tropics as seen by the TRMM precipitation radar. J. Clim. 16 (11), 1739–1756.

Schumacher, R.S., Johnson, R.H., 2005. Organization and environmental properties of extreme-rain-producing mesoscale convective systems. Mon. Weather Rev. 133 (4), 961–976.

Tramblay, Y., Somot, S., 2018. Future evolution of extreme precipitation in the Mediterranean. Clim. Chang. 151, 289–302. https://doi.org/10.1007/s10584-018-2300-5.

Turco, M., Llasat, M.C., 2011. Trends in indices of daily precipitation extremes in Catalonia (NE Spain), 1951–2003. Nat. Hazards Earth Syst. Sci. 11, 3213–3226. https://doi.org/10.5194/nhess-11-3213-2011.

Turco, M., Llasat, M.C., Herrera, S., Gutierrez, J.M., 2017. Bias Correction and Downscaling future RCM Precipitation Projections using a MOS-Analog Technique. J. Geophys. Res. Atmos. 122 https://doi.org/10.1002/2016JD025724.

Watson, P.A., Gunes, M., Potter, B.A., Sathiaseelan, V., Leitas, J., 1982. Development of a climatic map of rainfall attenuation for Europe. In: Final Report. ESA, ESTEC CONTR. No. 4162/79NL. Postgraduate School of Electronics and Electronic Engineering, University of Bradford, Bradford.

Weisman, M.L., Klemp, J.B., 1986. Characteristics of isolated convective storms. In: Ray, P.S. (Ed.), Mesoscale Meteorology and Forecasting. Am. Meteorol. Soc, pp. 331–358.

Westra, S., Fowler, H.J., Evans, J.P., Alexander, L.V., Berg, P., Johnson, F., Kendon, E.J., Lenderink, G., Roberts, N.M., 2014. Future changes to the intensity and frequency of short duration extreme rainfall. Rev. Geophys. 52, 522–555.

Wu, M., Luo, Y., Chen, F., Wong, W.K., 2019. Observed link of extreme hourly precipitation changes to urbanization over Coastal South China. J. Appl. Meteorol. Climatol. 58 (1799), 1819.

Ye, B., del Genio, A.D., Lo, K.K.-W., 1998. CAPE variations in the current climate and in a climate change. J. Clim. 11, 1997–2015.

Ye, H., Fetzer, E.J., Wong, S., Lambrigtsen, B.H., 2017. Rapid decadal convective precipitation increase over Eurasia during the last three decades of the 20th century. Sci. Adv. 2017, 3 e1600944. American Association for the Advancement of Science (AAAS), Washington, ISSN 2375-2548.